

# Constructing new pseudoscalar meson nonets with the observed $X(2100)$ , $X(2500)$ and $\eta(2225)$

Li-Ming Wang<sup>1,2,\*</sup>, Si-Qiang Luo<sup>1,2,†</sup>, Zhi-Feng Sun<sup>1,2,‡</sup> and Xiang Liu<sup>1,2§¶</sup>

<sup>1</sup>*School of Physical Science and Technology, Lanzhou University, Lanzhou 730000, China*

<sup>2</sup>*Research Center for Hadron and CSR Physics, Lanzhou University and Institute of Modern Physics of CAS, Lanzhou 730000, China*

(Dated: November 25, 2018)

Stimulated by the BESIII observation of  $\eta(2100)$ ,  $X(2500)$  and  $\eta(2225)$ , we try to pin down new pseudoscalar meson nonets with these states. The mass spectrum analysis and strong decay study indicate that  $X(2100)$  and  $\eta(2225)$  associated  $\pi(2070)$  and the predicate kaon  $K(2150)$  may form a new pseudoscalar meson nonet. In addition, more experimental data for  $X(2100)$  is needed to determine its structure. And then,  $X(2500)$  with  $X(2370)$ ,  $\pi(2360)$  and the predicted kaon  $K(2414)$  can be grouped into another new pseudoscalar meson nonet. These assignments to these discussed pseudoscalar states can be further tested in experiment since the predicted decay behaviors of these discussed states are given in this work.

PACS numbers: 14.40.Be, 13.25.Jx, 12.38.Lg

## I. INTRODUCTION

In the pseudoscalar meson family, the first nonet was constructed by  $\pi$ ,  $\eta(548)$ ,  $\eta'(958)$ , and  $K(494)$ , and then the second nonet appears with  $\pi(1300)$ ,  $\eta(1295)$ ,  $\eta(1475)$ , and  $K(1460)$ . Due to the study in Ref. [1], the observed  $X(1835)$  in the  $\eta'\pi^+\pi^-$  invariant mass spectrum of  $J/\psi \rightarrow \gamma\eta'\pi^+\pi^-$  associated with the  $\eta(1760)$ ,  $\pi(1800)$ , and  $K(1830)$  forms the third pseudoscalar meson nonet. By this way, one can categorize these observed pseudoscalar states into pseudoscalar meson family well. Obviously, it is not the end of this story.

In 2016, the BESIII Collaboration [2] performed a partial wave analysis of the  $J/\psi \rightarrow \gamma\phi\phi$  decay, by which two isoscalar pesudoscalar states  $X(2100)$  (in Ref. [2] it is named as  $\eta(2100)$ ) and  $X(2500)$  was observed with  $22\sigma$  significance and  $8.8\sigma$  significance, respectively. In addition,  $\eta(2225)$ , which was firstly reported in Ref. [3], was confirmed with  $28\sigma$  significance. The corresponding resonance parameters of them were measured [2], i.e.,

$$m_{X(2100)} = 2050^{+30+75}_{-24-26} \text{ MeV}, \quad (1)$$

$$\Gamma_{X(2100)} = 250^{+36+181}_{-30-164} \text{ MeV}, \quad (2)$$

$$m_{X(2500)} = 2470^{+15+101}_{-19-23} \text{ MeV}, \quad (3)$$

$$\Gamma_{X(2500)} = 230^{+64+56}_{-35-33} \text{ MeV}, \quad (4)$$

$$m_{\eta(2225)} = 2216^{+4+21}_{-5-11} \text{ MeV}, \quad (5)$$

$$\Gamma_{\eta(2225)} = 185^{+12+43}_{-14-17} \text{ MeV}. \quad (6)$$

These newly observed  $X(2500)$ ,  $X(2100)$  and  $\eta(2225)$  provide us good chance to construct new pseudoscalar

meson nonets with higher radial excitation. Just considering this point, in this work we study whether the newly observed  $X(2500)$ ,  $X(2100)$  and  $\eta(2225)$  can be categorized into pseudoscalar meson nonets. Firstly, we perform an analysis of the Regge trajectories, which provides important hint of how to group these pseudoscalar states into new pseudoscalar meson family. Secondly, we study their two-body strong decays by the flux-tube model, which can be applied to test these possible assignments. In the next sections, we will give detailed illustration.

When constructing pseudoscalar meson nonets with higher radial excitation, the corresponding pseudoscalar kaons are still missing in experiment. Thus, as a important theoretical predication, the masses and the decay behaviors of kaons in constructing pseudoscalar meson nonets will be given here, which is helpful to future experimental search for them.

This paper is organized as follows. After introduction, we concisely review the research status of the reported pseudoscalar states above 2 GeV in Sec. II. And then, we present mass spectrum analysis by the approach of the Regge trajectories in Sec. III. The two-body decay behaviors of these discussed pseudoscalar states are given in Sec. IV. The paper ends with the short summary.

## II. A CONCISE REVIEW OF THE REPORTED PSEUDOSCALAR STATES ABOVE 2 GEV

Before the BESIII's analysis, several isoscalar pseudoscalar states were reported [1, 2, 4, 7, 8, 10, 13, 21–23, 34, 48], which include  $\eta(2010)$ ,  $\eta(2100)$ ,  $\eta(2190)$ ,  $\eta(2320)$ ,  $X(2120)$ , and  $X(2370)$ . However, these isoscalar pseudoscalar states were not listed in summary meson table of the Particle Data Group (PDG) [5] since they were not confirmed by other experiments. It also means that  $\eta(2010)$ ,  $\eta(2100)$ ,  $\eta(2190)$ ,  $\eta(2320)$ ,  $X(2120)$ , and  $X(2370)$  were not established in experiment. The

<sup>§</sup>Corresponding author

<sup>\*</sup>Electronic address: lmwang15@lzu.edu.cn

<sup>†</sup>Electronic address: luosq15@lzu.edu.cn

<sup>‡</sup>Electronic address: sunzhif09@lzu.edu.cn

<sup>¶</sup>Electronic address: xiangliu@lzu.edu.cn

$\eta(2010)$  with mass  $2010^{+35}_{-60}$  MeV and width  $270 \pm 60$  MeV was found by analyzing  $p\bar{p}$  annihilation into  $\eta\pi^0\pi^0$ ,  $\pi^0\pi^0$ ,  $\eta\eta$  and  $\pi^-\pi^+$  [4].  $\eta(2100)$  was observed by the DM2 experiment in the radiative decay  $J/\psi \rightarrow \gamma\rho\rho$  [7]. In Ref. [48], the  $\eta(2190)$  was introduced by studying the data of the radiative decays of  $J/\psi$  into the  $0^-$  final states [44], which has mass  $2190 \pm 50$  MeV and width  $850 \pm 100$  MeV. In Ref. [10], the authors discussed the possibility of the  $\eta(2010)$  and  $\eta(2190)$  as  $4^1S_0$  isoscalar states. The  $\eta(2225)$  was suggested to be a good candidate for the  $4^1S_0 s\bar{s}$  state [11]. The  $\eta(2100)$  and  $\eta(2225)$  were treated as the third radial excitation of  $\eta$  and  $\eta'$ , respectively in Ref. [10].  $\eta(2320)$  was discovered from the combined analysis of  $p\bar{p} \rightarrow \eta\eta\eta$  and  $p\bar{p} \rightarrow \eta\pi\pi$  [12]. The  $X(2120)$  and  $X(2370)$  are two pseudoscalar states observed by BESIII in the invariant mass spectrum of the  $J/\psi \rightarrow \eta'\pi^+\pi^-$  decay [8]. The observation of the  $X(2120)$  and  $X(2370)$  also stimulated the discussions of them as pseudoscalar meson, glueball and hadronic molecular state [1, 13, 21, 22]. In Ref. [21], the author has studied the mass spectrum of baryonium with the Bethe-Salpeter equation [15–19], and  $X(2370)$  can be identified as  $p\bar{N}(1400)$  bound state.

Besides these isoscalar pseudoscalar states mentioned above, there are two isovector pseudoscalar states  $\pi(2360)$  and  $\pi(2070)$  above 2 GeV, which were observed by the Crystal Barrel experiment, where the partial wave analysis of the decay  $p\bar{p} \rightarrow \eta\eta\pi^0$  was performed [20]. The  $\pi(2360)$  has mass  $M = 2360 \pm 25$  MeV and width  $\Gamma = 300^{+100}_{-50}$  MeV, while the  $\pi(2070)$  has mass  $M = 2070 \pm 35$  MeV and width  $\Gamma = 310^{+100}_{-50}$  MeV. Anisovich *et al.* suggested  $\pi(2360)$  and  $\pi(2070)$  as the third and the fourth radial excitations of  $\pi$  meson family, respectively [46]. In Ref [10], the two-body strong decays of the  $\pi(2070)$  are calculated by the quark pair creation model if treating the  $\pi(2070)$  as  $\pi(4S)$ . The  $\pi(2360)$  as  $\pi(5^1S_0)$  was supported by the analysis of Regge trajectories [23].

From this concise review of these observed pseudoscalar states above 2 GeV, we can learn that the experimental and theoretical studies are still mess, especially for these isoscalar pseudoscalar states. In the following, we try to establish new pseudoscalar meson nonets with higher radial excitation by combining the newly observed  $X(2100)$ ,  $X(2500)$  and  $\eta(2225)$  by BESIII with these reported pseudoscalar states.

### III. MASS SPECTRUM ANALYSIS

In the light pseudoscalar sector,  $\eta$  and  $\eta'(958)$  together with  $\pi$  and  $K$  can be elements of meson nonet well, while  $\eta(1475)$ ,  $\eta(1295)$ ,  $K(1460)$  and  $\pi(1300)$  form the meson nonet with the first radial excitation. In Refs. [1, 13, 14, 21, 31, 46],  $X(1835)$ ,  $\eta(1760)$ ,  $K(1830)$  and  $\pi(1800)$  are depicted as the states with quantum number  $3^1S_0$ . What we will discuss in this paper are the third and fourth radial excitation pseudoscalar mesons.

Regge trajectory analysis [24, 25] is a practical way to study the mass spectrum [26–29] of mesons. The relation between mass and radial quantum number  $n$  is

$$M^2 = M_0^2 + (n-1)\mu^2, \quad (7)$$

where  $M_0$  and  $M$  are the masses of ground state and  $(n-1)$ th radial excitation state, respectively.  $\mu^2$  denotes the slope of the trajectory with the value  $\mu^2 = 1.25 \pm 0.15$  GeV<sup>2</sup> [30].

We plot the Regge trajectories in Fig. 1. We notice that  $\pi(2070)$ ,  $\pi(2360)$  as  $4^1S_0$  and  $5^1S_0$  states respectively together with  $\pi$ ,  $\pi(1300)$  and  $\pi(1800)$  populate a common trajectory. For  $\eta(4S)$ , the predicted mass by the analysis of Regge trajectories is about 2064 MeV, where  $\eta(2010)$ ,  $\eta(2100)$ ,  $\eta(2190)$ ,  $X(2100)$  and  $X(2120)$  are its candidates. Similarly,  $X(2370)$ ,  $\eta(2225)$  and  $X(2500)$  are candidates for  $\eta(5S)$ ,  $\eta'(4S)$  and  $\eta'(5S)$ , respectively. The former theoretical studies on the mass of  $\pi(4S)$ ,  $\eta(4S)$ ,  $\eta'(4S)$ ,  $\pi(5S)$ ,  $\eta(5S)$ ,  $\eta'(5S)$  [10, 23, 30, 32, 46, 47, 49, 50, 60] are consistent with the trajectory analysis in our work.

For the sake of completeness, the kaons with higher radial excitation should appear in the corresponding nonets. However, there is no experimental information about them with quantum numbers  $4^1S_0$  and  $5^1S_0$ . With the help of diagonalization of the mass squared matrix and Gell-Mann-Okubo mass formula, the following relation is obtained [10]

$$\begin{aligned} & 8X^2(M_{K(n^1S_0)}^2 - M_{\pi(n^1S_0)}^2)^2 \\ &= [4M_{K(n^1S_0)}^2 - (2-X^2)M_{\pi(n^1S_0)}^2 - (2+X^2) \\ &\quad \times M_{X(n^1S_0)}^2][(2-X^2)M_{\pi(n^1S_0)}^2 + (2+X^2) \\ &\quad \times M_{X(n^1S_0)}^2 - 4M_{K(n^1S_0)}^2], \end{aligned} \quad (8)$$

where  $X$  describes the SU(3)-breaking ratio of the non-strange and strange quark propagators via the constituent quark mass ratio  $m_u/m_s$ . The masses of  $K(4^1S_0)$  and  $K(5^1S_0)$  are predicted to be 2150 and 2414 MeV, respectively, so that we label them as  $K(2150)$  and  $K(2414)$ , respectively. In addition, these two states are approximately located at the trajectory for kaons.

Only the mass information is not sufficient to classify the structure of the states mentioned above. So, we study the two-body strong decay of them in the next section.

### IV. TWO-BODY STRONG DECAY BEHAVIORS

#### A. A brief introduction of the flux-tube model

In this paper, we study the strong decay behavior of the third and fourth radial excitation pseudoscalar meson nonets by the flux-tube model [33–38]. In the following, a brief introduction of this model is given.

The flux-tube model, first proposed by Isgur and Paton, is an useful tool for describing the decay properties

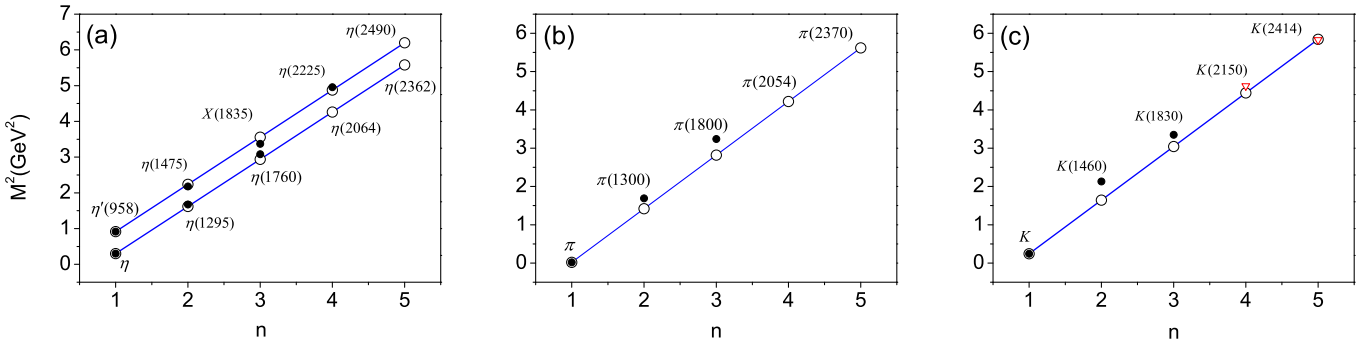


FIG. 1: (color online). The Regge trajectories for the  $\eta/\eta'$ ,  $\pi$  and  $K$  mass spectrum with  $\mu^2 = 1.32 \text{ GeV}^2$ ,  $1.40 \text{ GeV}^2$ ,  $1.40 \text{ GeV}^2$  respectively. Here,  $\circ$  denotes Regge trajectories theoretical values.  $\nabla$  denotes theoretical values from Gell-Mann-Okubo mass formula [10]. And  $\bullet$  denotes experimental values from PDG [5].

of hadrons. It is suggested by the strong coupling limit of Hamiltonian lattice QCD. In this model, a meson composed of a quark and an antiquark are connected by a tube of chromoelectric flux. Here, the flux tube can be treated as a vibrating string. Fig. 2 describes the picture of a meson decay, which happens when the string breaks at a point, and then the free ends of the flux tube for initial meson (i.e.,  $q_i$  and  $\bar{q}_i$ ) connect to the quark-antiquark pair created from the vacuum.

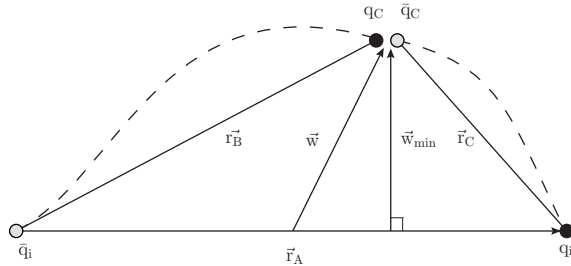


FIG. 2: The position-space coordinates used in the flux-tube model.

In this paper, within the frame of flux-tube model, the expression of partial wave amplitude is

$$\begin{aligned} \mathcal{M}^{SL}(P) = & \gamma_0 \frac{\sqrt{32\pi(2L+1)E_A E_B E_C}}{2J_A+1} \sum_{\substack{M_{LA}, M_{SA}, M_{LB}, M_{SB}, \\ M_{LC}, M_{SC}, M_{JB}, M_{JC}, m}} \\ & \times \langle L0S(M_{JB} + M_{JC}) | J_A(M_{JB} + M_{JC}) \rangle \\ & \times \langle J_B M_{JB} J_C M_{JC} | S(M_{JB} + M_{JC}) \rangle \\ & \times \langle L_A M_{LA} S_A M_{SA} | J_A(M_{JB} + M_{JC}) \rangle \\ & \times \langle L_B M_{LB} S_B M_{SB} | J_B M_{JB} \rangle \langle L_C M_{LC} S_C M_{SC} | J_C M_{JC} \rangle \\ & \times \langle 1m1 - m|00 \rangle \langle \chi_{S_B M_{SB}}^{14} \chi_{S_C M_{SC}}^{32} | \chi_{S_A M_{SA}}^{12} \chi_{1-m}^{34} \rangle \\ & \times [\langle \phi_B^{14} \phi_C^{32} | \phi_A^{12} \phi_0^{34} \rangle I^{\text{ft}}(P\hat{z}, m_1, m_2, m_3) \\ & + (-1)^{L_A+L_B+L_C+S_A+S_B+S_C} \langle \phi_B^{32} \phi_C^{14} | \phi_A^{12} \phi_0^{34} \rangle \\ & \times I^{\text{ft}}(P\hat{z}, m_2, m_1, m_3)], \end{aligned} \quad (9)$$

where the coordinate space integral is shown as follows

$$\begin{aligned} I^{\text{ft}}(\vec{P}, m_1, m_2, m_3) = & -\frac{8}{(2\pi)^{3/2}} \int d^3\vec{r} \int d^3\vec{w} \\ & \times \psi_{n_B L_B M_{LB}}^*(-\vec{w} - \vec{r}) \psi_{n_C L_C M_{LC}}^*(\vec{w} - \vec{r}) \\ & \times y_1^m \left( \left[ (\vec{P} + i\vec{\nabla}_{\vec{r}_A}) \psi_{n_A L_A M_{LA}}(\vec{r}_A) \right]_{\vec{r}_A=-2\vec{r}} \right) \\ & \times \exp(-\frac{1}{2}bw_{\min}^2) \exp(i\vec{P} \cdot (m_+ \vec{r} + m_- \vec{w})) \end{aligned} \quad (10)$$

with  $m_+ = \frac{m_1}{m_1+m_3} + \frac{m_2}{m_2+m_3}$ ,  $m_- = \frac{m_1}{m_1+m_3} - \frac{m_2}{m_2+m_3}$ . In Eq. (9),  $\gamma_0$  is a new phenomenological parameter, which can be fixed as 14.8 by fitting the experimental data from PDG (see Table I).  $b$  is the string tension which has the typical value  $0.18 \text{ GeV}^2$ . And  $w_{\min}$  is shortest distance from a point, where the quark-antiquark pair is created from vacuum to the segment connected original quark and antiquark in initial state. The expression of  $w_{\min}^2$  reads

$$w_{\min}^2 = \begin{cases} w^2 \sin^2 \theta & \text{if } r \geq w | \cos \theta | \\ r^2 + w^2 - 2rw | \cos \theta | & \text{if } r < w | \cos \theta | \end{cases}. \quad (11)$$

And then, one can get the decay width

$$\Gamma = \frac{\pi}{4} \frac{|\mathbf{P}|}{M_A^2} \sum_{LS} |\mathcal{M}^{LS}|^2, \quad (12)$$

where  $\mathbf{P}$  is momentum of meson  $B$ ,  $L$  denotes relative orbital angular momentum between mesons  $B$  and  $C$ .  $S$  is total spin of  $B$  and  $C$ . In order to simplify the calculation, we use the harmonic oscillator wave function to depict the meson, which reads

$$\psi_{nL M_L}(\mathbf{r}) = R_{nL}^{\text{SHO}}(r) Y_{LM_L}(\Omega_r) \quad (13)$$

with the radial wave function

$$\begin{aligned} R_{nL}^{\text{SHO}}(r) = & \frac{1}{R^{3/2}} \sqrt{\frac{2n!}{\Gamma(n+L+3/2)}} \left( \frac{r}{R} \right)^L \\ & \times e^{-\frac{r^2}{2R^2}} L_n^{L+1/2}(r^2/R^2). \end{aligned} \quad (14)$$

Here,  $L_n^{L+1/2}(r^2/R^2)$  is an associated Laguerre polynomial. The parameter  $R$  is determined by reproducing the realistic root mean square radius by solving the *Schrödinger* equation with the linear potential plus color Coulomb and Gaussian-smeared contact hyperfine term [40]. The  $R$  value can be obtained through the relation [41, 42]

$$\int |\psi_{nLM_L}^{\text{SHO}}(\mathbf{r})|^2 r^2 d^3\mathbf{r} = \int |\Phi(\mathbf{r})|^2 r^2 d^3\mathbf{r}. \quad (15)$$

The  $\Phi(\mathbf{r})$  is the wave function of a certain meson in the potential model [43].

TABLE I: The measured partial decay widths of 10 decay channels and the comparison with theoretical calculation

Decay channel	Experiment (MeV) [5]	Our fit (MeV)
$\rho \rightarrow \pi\pi$	147.8	83.3
$b_1(1235) \rightarrow \omega\pi$	142	129.5
$f_2(1270) \rightarrow \pi\pi$	156.5	85.1
$f'_2 \rightarrow K\bar{K}$	64.8	90.6
$K^* \rightarrow K\pi$	50.8	34.9
$K_0^*(1430) \rightarrow K\pi$	251	381.3
$K_2^*(1430) \rightarrow K\pi$	49.1	63.9
$K_2^*(1430) \rightarrow K^*\pi$	24.3	33.8
$K_3^*(1780) \rightarrow K^*\pi$	49.3	42.6
$K_3^*(1780) \rightarrow K\pi$	28.6	46.5

## B. The fourth pseudoscalar meson nonet

As discussed in Sec. III,  $\eta(2010)$ ,  $\eta(2100)$ ,  $X(2120)$  and  $\eta(2190)$  can be regarded as the candidates of the third radial excitation of  $\eta(548)$ , while  $\eta(2225)$  is the candidate of  $\eta'(4S)$ . Besides,  $\pi(2070)$  can be a  $4^1S_0$  state. We also analyze the mass of third radial excitation of kaon, which is around 2151 MeV and labeled as  $K(2150)$  here. In Tables II and III, the decay channels are listed. In the following, we present the strong decay properties of these particles.

In Fig. 3, we show the total and partial decay widths of  $\pi(2070)$  as a  $4^1S_0$  state. Comparing our theoretical result with the experimental data, we get that the  $R$  value lies in the range  $5.55 \sim 5.81 \text{ GeV}^{-1}$ , which is consistent with that in Ref. [46].  $\rho\pi$  is the dominant decay channel with width 233 MeV. Here, we choose the typical value of  $R$  as  $5.65 \text{ GeV}^{-1}$ , by which the center value of the experimental data can be reproduced.  $KK^*$  and  $\eta a_0(1450)$  are other two sizable decay modes, with the widths 18.22 and 14.38 MeV respectively. The partial width of  $\rho(1450)\pi$ ,  $\rho a_1(1260)$ ,  $\rho\omega$  are very sensitive to the  $R$  value due to the node effect.

The decay width of  $X(2100)$  depending on  $R$  is shown in Fig. 4. We can not conclude whether or not  $X(2100)$  is the  $\eta(4S)$ , since the error of experimental width is too

large. From Fig. 4, we can see that  $\pi a_0(1450)$  is the dominant channel. So we suggest further experiments could study the property of  $X(2100)$  via  $\pi a_0(1450)$  decay mode. In addition, we also study the strong decay of  $\eta(2010)$ ,  $\eta(2100)$ ,  $X(2120)$  and  $\eta(2190)$  under the assignment of third excitation of  $\eta(548)$ . Our results indicate that  $\eta(2010)$ ,  $\eta(2100)$  and  $\eta(2190)$  as the  $4^1S_0$  isoscalar state are unfavored, whereas  $X(2120)$  seems plausible as the candidate of the  $4^1S_0$  isoscalar state.

As mentioned above,  $\eta(2225)$  is a good candidate of  $\eta'(4S)$ . The plot of decay width as a function of  $R$  is shown in Fig. 5. The  $R$  value is between  $5.01 \text{ GeV}^{-1}$  and  $5.32 \text{ GeV}^{-1}$ , which gives an overlap of theoretical and experimental data. The plausible range of  $R$  agrees with that in Ref. [22]. The main decay channels are  $KK^*$ ,  $KK_0^*(1430)$ , which have the partial widths of 147 and 36.67 MeV, respectively.  $KK^*(1410)$ ,  $KK_2^*(1430)$  and  $K^*K^*$  are highly suppressed due to node effect. The width of its  $\phi\phi$  channel is not ignorable, which can naturally explain why  $\eta(2225)$  is observed by BES via  $J/\psi \rightarrow \gamma\phi\phi$  [3].

For kaon  $K(2150)$  with  $4^1S_0$ , there is no experimental information at present. The mass of it is about 2151 MeV. In Fig. 6, we show the strong decay width of this state, from which we see that the dominant modes are  $\pi K^*$ ,  $\rho K$ . We suggest that the experiments to search for  $K(2150)$  via these decay channels.

## C. The fifth pseudoscalar meson nonet

In the following, we will study the strong decay of the fourth pseudoscalar meson nonet. In Tables II and III, the OZI-allowed decay channels are listed.

$\pi(2360)$  is a good candidate of  $5^1S_0$  state. In Fig. 7, we plot the decay width of  $\pi(2360)$  depending on  $R$ . Comparing to the experimental data, we get the value of  $R$  lying in the range  $5.43 \sim 5.65 \text{ GeV}^{-1}$ , which is in agreement with that in Ref. [46]. Its dominant decay channel is  $\rho\pi$  with width 205 MeV. In addition, other channels such as  $\rho(1450)\pi$ ,  $KK^*$ ,  $\rho a_1(1260)$  and  $\pi f_2(1270)$  are also important.

The Regge trajectory analysis shows that  $X(2370)$  and  $\eta(2320)$  can be candidates of the fourth radial excitation of  $\eta(548)$ . However, our calculation demonstrates that  $\eta(2320)$  can not be  $\eta(5S)$ , since we can not produce the experimental width of  $\eta(2320)$  under this assignment. Under the assignment of  $\eta(5S)$  meson, we can get the width of  $X(2370)$  which is shown in Fig. 8. If choosing  $R$  around  $5.44 \text{ GeV}^{-1}$  which is similar to Ref. [1], the theoretical value of the total width equals to the experimental central value. From Fig. 8, we can see that the  $\rho\rho$ ,  $KK^*$ ,  $\pi a_0(1450)$ ,  $a_0(980)\pi(1300)$ ,  $\pi a_2(1320)$  and  $\rho b_1(1235)$  channels are important.

According to the mass spectrum analysis,  $X(2500)$  is a good candidate of  $\eta'(5S)$ . In Fig. 9, we plot the decay width of  $X(2500)$  under the assignment of fourth radial excitation of  $\eta'(958)$ . The value of  $R$  corresponding to

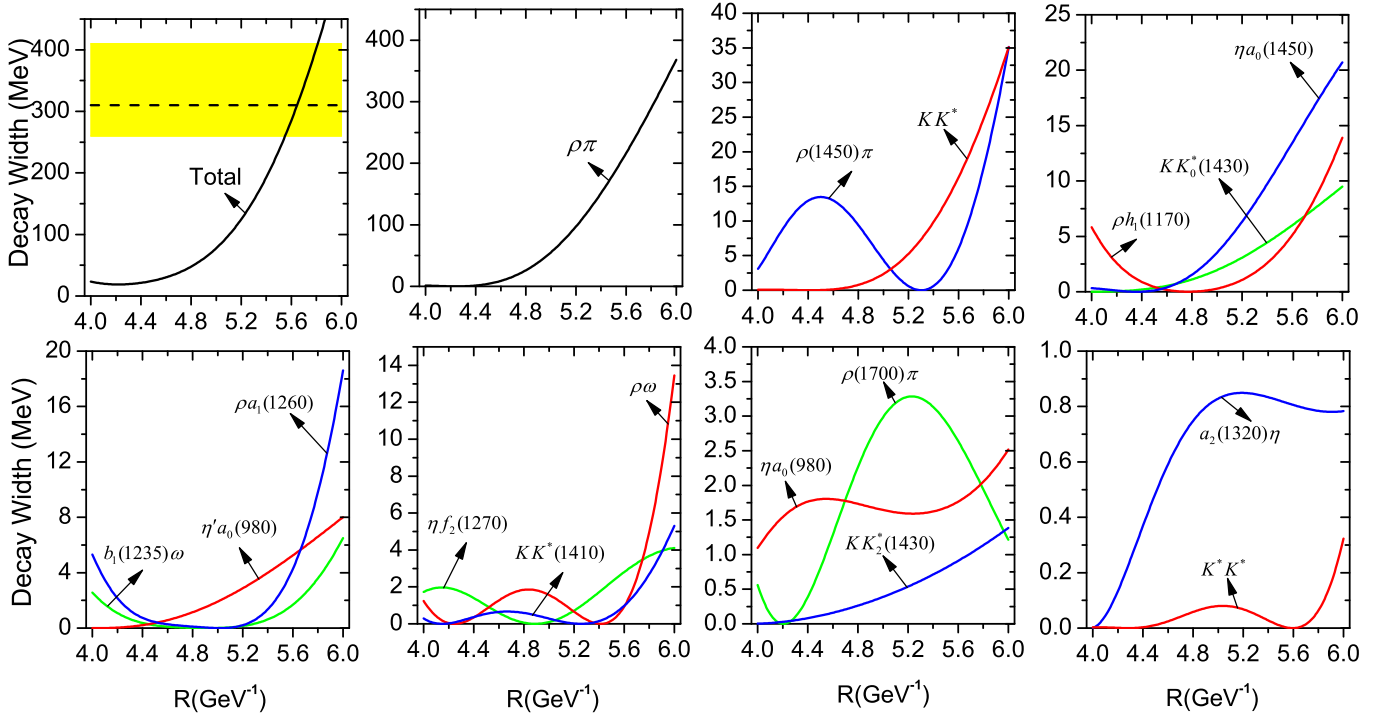


FIG. 3: (color online). The  $R$  dependence of two-body strong decay widths of  $\pi(2070)$  as  $\pi(4S)$  state. The experimental data is marked by the yellow band. Some tiny channels are not drawn up.

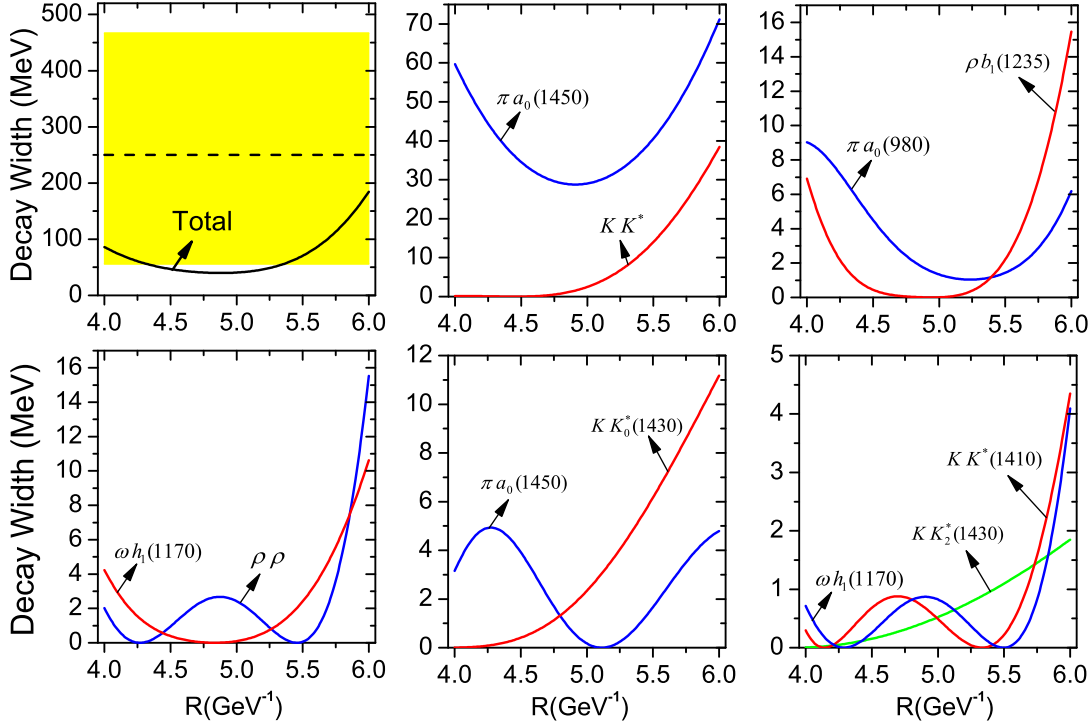


FIG. 4: (color online). The  $R$  dependence of total decay width and partial two-body decay width of  $X(2100)$  as the third radial excitation of  $\eta$ . The experimental data is marked by the yellow band. Some tiny channels are not drawn up. Here, the mixing angle we take is  $-2.61^\circ$ .

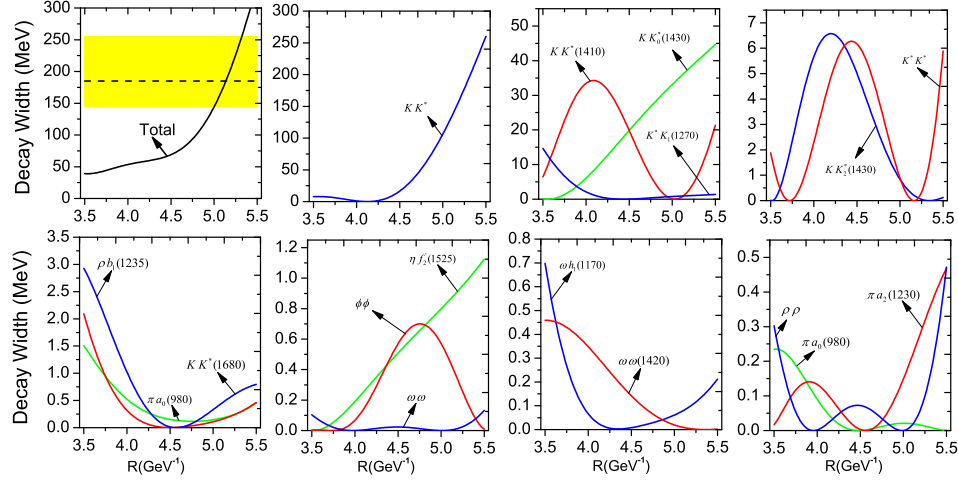


FIG. 5: (color online). The  $R$  dependence of total decay width and partial two-body decay width of  $\eta(2225)$  as the third radial excitation of  $\eta$ . The experimental data is marked by the yellow band. Some tiny channels are not drawn up. Here, the mixing angle we take is  $6.93^\circ$ .

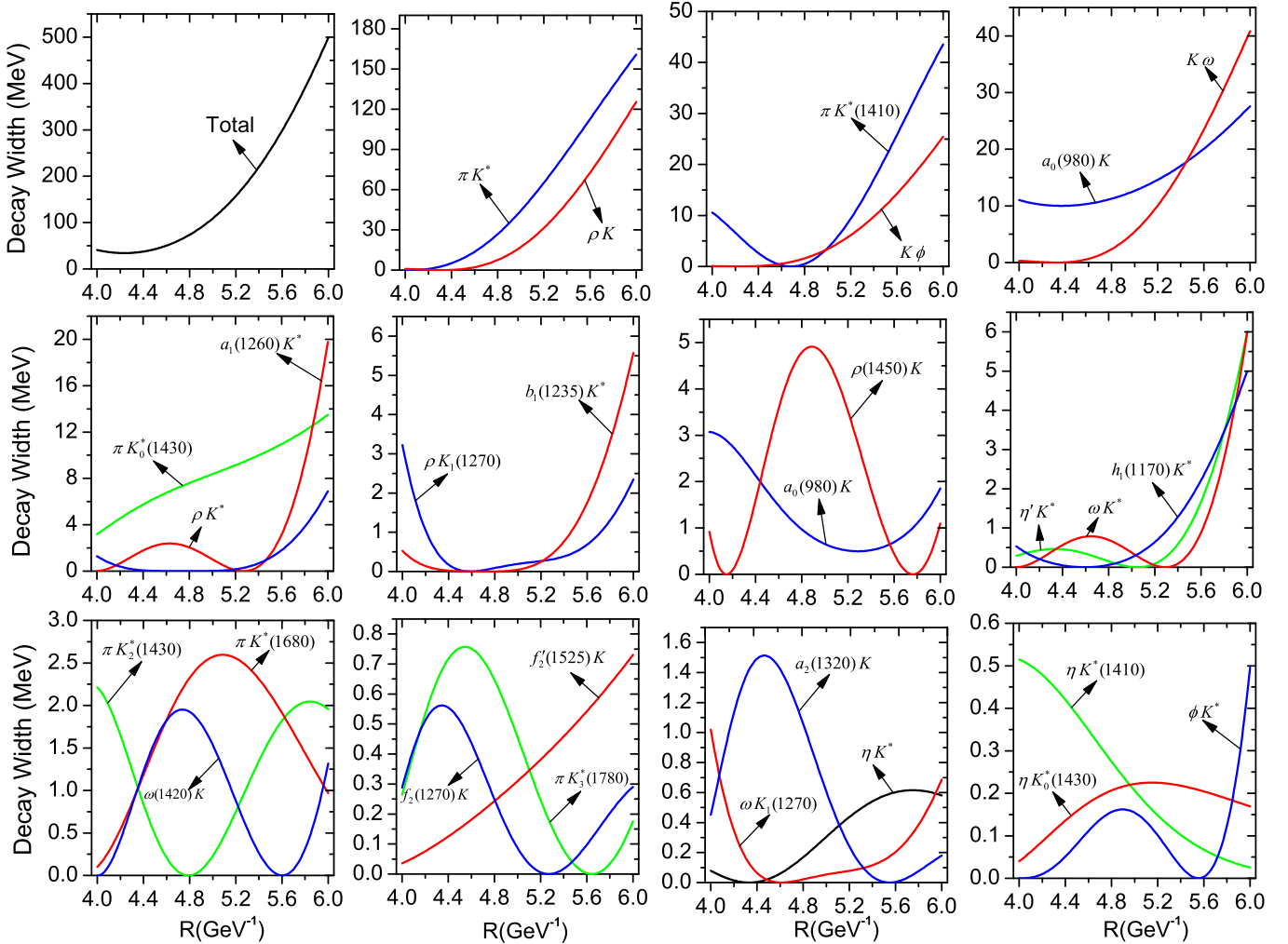


FIG. 6: (color online). The  $R$  dependence of two-body decay widths of  $K(2150)$  as the third radial excitation of  $K$ . Some tiny channels are not drawn up.

TABLE II: The allowed two-body decays of  $X(2100)$ ,  $\eta(2225)$ ,  $X(2370)$ ,  $X(2500)$ ,  $\pi(2070)$  and  $\pi(2360)$  are marked by  $\checkmark$ . Here,  $\rho$ ,  $\phi$ ,  $\omega$  denote  $\rho(770)$ ,  $\phi(1020)$ ,  $\omega(782)$ .

Modes	Channel	$X(2100)$	$\eta(2225)$	$X(2370)$	$X(2500)$	Channel	$\pi(2070)$	$\pi(2360)$
$0^- + 0^+$	$\pi a_0(980)$	$\checkmark$	$\checkmark$	$\checkmark$	$\checkmark$	$\eta a_0(980)$	$\checkmark$	$\checkmark$
	$\pi a_0(1450)$	$\checkmark$	$\checkmark$	$\checkmark$	$\checkmark$	$\eta a_0(1450)$	$\checkmark$	$\checkmark$
	$\pi(1300) a_0(980)$			$\checkmark$	$\checkmark$	$\eta' a_0(980)$	$\checkmark$	$\checkmark$
	$K K_0^*(1430)$	$\checkmark$	$\checkmark$	$\checkmark$	$\checkmark$	$\eta(1295) a_0(980)$	$\checkmark$	
$1^- + 1^+$	$\rho b_1(1235)$	$\checkmark$	$\checkmark$	$\checkmark$	$\checkmark$	$\rho(770) h_1(1170)$	$\checkmark$	$\checkmark$
	$\omega h_1(1170)$	$\checkmark$	$\checkmark$	$\checkmark$	$\checkmark$	$\rho(770) h_1(1380)$		$\checkmark$
	$\phi h_1(1170)$		$\checkmark$	$\checkmark$	$\checkmark$	$\omega(782) b_1(1235)$	$\checkmark$	$\checkmark$
	$\phi h_1(1380)$				$\checkmark$	$K^* K_1(1270)$		$\checkmark$
	$K^* K_1(1270)$			$\checkmark$	$\checkmark$	$K^* K_1(1400)$		$\checkmark$
	$K^* K_1(1400)$			$\checkmark$	$\checkmark$	$\rho(770) a_1(1260)$	$\checkmark$	$\checkmark$
$0^- + 1^-$	$K K^*(1410)$	$\checkmark$	$\checkmark$	$\checkmark$	$\checkmark$	$K K^*$	$\checkmark$	$\checkmark$
	$K K^*$	$\checkmark$	$\checkmark$	$\checkmark$	$\checkmark$	$K K^*(1410)$	$\checkmark$	$\checkmark$
	$K K^*(1680)$		$\checkmark$	$\checkmark$	$\checkmark$	$K K^*(1680)$		$\checkmark$
	$K(1460) K^*$			$\checkmark$	$\checkmark$	$K(1460) K^*$		$\checkmark$
						$\pi \rho(770)$	$\checkmark$	$\checkmark$
						$\pi \rho(1450)$	$\checkmark$	$\checkmark$
						$\pi \rho(1700)$	$\checkmark$	$\checkmark$
						$\pi(1300) \rho(770)$		$\checkmark$
$0^+ + 1^+$	$a_0(980) a_1(1260)$			$\checkmark$	$\checkmark$	$a_0(980) f_1(1285)$		$\checkmark$
						$a_0(980) b_1(1235)$		$\checkmark$
$1^- + 1^-$	$\rho \rho$	$\checkmark$	$\checkmark$	$\checkmark$	$\checkmark$	$\rho(770) \omega(782)$	$\checkmark$	$\checkmark$
	$\rho \rho(1450)$		$\checkmark$	$\checkmark$	$\checkmark$	$\rho(770) \omega(1420)$	$\checkmark$	$\checkmark$
	$\omega \omega$	$\checkmark$	$\checkmark$	$\checkmark$	$\checkmark$	$\omega(782) \rho(1450)$		$\checkmark$
	$\omega \omega(1420)$		$\checkmark$	$\checkmark$	$\checkmark$	$K^* K^*$	$\checkmark$	$\checkmark$
	$\phi \phi$	$\checkmark$	$\checkmark$	$\checkmark$	$\checkmark$	$K^* K^*(1410)$		$\checkmark$
	$K^* K^*$	$\checkmark$	$\checkmark$	$\checkmark$	$\checkmark$			
	$K^* K^*(1410)$			$\checkmark$	$\checkmark$			
$0^- + 2^+$	$\pi a_2(1320)$	$\checkmark$	$\checkmark$	$\checkmark$	$\checkmark$	$\pi f_2(1270)$	$\checkmark$	$\checkmark$
	$\pi a_2(1700)$	$\checkmark$	$\checkmark$	$\checkmark$	$\checkmark$	$\eta a_2(1320)$	$\checkmark$	$\checkmark$
	$\eta f_2(1270)$	$\checkmark$	$\checkmark$	$\checkmark$	$\checkmark$	$\eta a_2(1700)$		$\checkmark$
	$\eta f'_2(1270)$		$\checkmark$	$\checkmark$	$\checkmark$	$\eta' a_2(1320)$		$\checkmark$
	$\eta' f_2(1270)$			$\checkmark$	$\checkmark$	$K K_2^*(1430)$	$\checkmark$	$\checkmark$
	$K K_2^*(1430)$	$\checkmark$	$\checkmark$	$\checkmark$	$\checkmark$			
$1^- + 2^+$	$K^* K_2^*(1430)$			$\checkmark$	$\checkmark$	$K^* K_2^*(1430)$		$\checkmark$
						$\rho(770) a_2(1320)$		$\checkmark$
$0^- + 3^-$	$K K_3^*(1780)$			$\checkmark$	$\checkmark$	$K K_3^*(1780)$		$\checkmark$
$0^- + 4^+$	$\pi a_4(2030)$		$\checkmark$	$\checkmark$	$\checkmark$			

central value of experimental width falls in the range of  $4.98 \sim 5.32 \text{ GeV}^{-1}$ . If choosing a typical value of  $R$  as  $5.13 \text{ GeV}^{-1}$ , the dominant decay modes  $KK^*$  have the width of 154 MeV. Besides,  $\phi\phi$  channel is not ignorable, which can explain why  $X(2500)$  is observed in  $\phi\phi$  channel.

As mentioned in Sec. III, the  $5^1S_0$  state of kaon which is labeled by  $K(2414)$  has a mass of 2414 MeV. The strong decay, which is shown in Fig. 10, is dominant

by  $\pi K^*$  and  $\rho K$ . Additionally,  $\pi K^*(1410)$ ,  $K\phi$ ,  $K\omega$ ,  $a_0(980)K$  are also important. This result will be helpful to explore  $K(2414)$  in experiment.

## V. DISCUSSION AND CONCLUSION

Inspired by the observed  $\eta(2100)$ ,  $X(2500)$  and  $\eta(2225)$ , we try to construct new pseudoscalar meson

TABLE III: The allowed two-body decays of  $K(2150)$  and  $K(2414)$  are marked by  $\checkmark$ . Here,  $\rho, \phi, \omega$  denote  $\rho(770), \phi(1020), \omega(782)$ , respectively.

Channel	$K(2150)$	$K(2414)$	Channel	$K(2150)$	$K(2414)$
$\pi K_0^*(1430)$	$\checkmark$	$\checkmark$	$\eta K_0^*(1430)$	$\checkmark$	$\checkmark$
$\eta^* K_0^*(1430)$		$\checkmark$	$K a_0(980)$	$\checkmark$	$\checkmark$
$K a_0(1450)$		$\checkmark$	$\rho K_1(1270)$	$\checkmark$	$\checkmark$
$\rho K_1(1400)$		$\checkmark$	$\omega K_1(1270)$	$\checkmark$	$\checkmark$
$\omega K_1(1400)$		$\checkmark$	$\phi K_1(1270)$		$\checkmark$
$K^* h_1(1170)$	$\checkmark$	$\checkmark$	$K^* h_1(1380)$		$\checkmark$
$K^* b_1(1235)$	$\checkmark$	$\checkmark$	$K^* a_1(1260)$		$\checkmark$
$K^* f_1(1285)$		$\checkmark$	$K^* f_1(1420)$		$\checkmark$
$\pi K^*$	$\checkmark$	$\checkmark$	$\pi K^*(1410)$	$\checkmark$	$\checkmark$
$\pi K^*(1680)$		$\checkmark$	$\eta K^*$	$\checkmark$	$\checkmark$
$\eta K^*(1410)$	$\checkmark$	$\checkmark$	$\eta K^*(1680)$		$\checkmark$
$\eta' K^*$	$\checkmark$	$\checkmark$	$\eta' K^*(1410)$	$\checkmark$	$\checkmark$
$\pi(1300) K^*$		$\checkmark$	$K \rho$	$\checkmark$	$\checkmark$
$K \omega$	$\checkmark$	$\checkmark$	$K \phi$	$\checkmark$	$\checkmark$
$K \omega(1420)$	$\checkmark$	$\checkmark$	$K \rho(1450)$	$\checkmark$	$\checkmark$
$K \omega(1650)$	$\checkmark$	$\checkmark$	$K \phi(1680)$		$\checkmark$
$K(1460) \rho$		$\checkmark$	$K(1460) \omega$		$\checkmark$
$a_0(980) K_1(1270)$		$\checkmark$	$a_0(980) K_1(1400)$		$\checkmark$
$\rho K^*$	$\checkmark$	$\checkmark$	$\rho K^*(1410)$		$\checkmark$
$\omega K^*$	$\checkmark$	$\checkmark$	$\omega K^*(1410)$		$\checkmark$
$\phi K^*$	$\checkmark$	$\checkmark$	$\rho(1450) K^*$		$\checkmark$
$\omega(1420) K^*$		$\checkmark$	$K f_2(1270)$	$\checkmark$	$\checkmark$
$K a_2(1320)$	$\checkmark$	$\checkmark$	$K f'_2(1525)$	$\checkmark$	$\checkmark$
$K a_2(1700)$		$\checkmark$	$\pi K_2^*(1430)$	$\checkmark$	$\checkmark$
$\eta K_2^*(1430)$	$\checkmark$	$\checkmark$	$\eta' K_2^*(1430)$		$\checkmark$
$K^* f_2(1270)$		$\checkmark$	$K^* a_2(1320)$		$\checkmark$
$\omega K_2^*(1430)$		$\checkmark$	$\rho K_2^*(1430)$		$\checkmark$
$\pi K_3^*(1680)$		$\checkmark$	$\eta K_3^*(1680)$		$\checkmark$

nonets with these states.  $\pi$ ,  $K$ ,  $\eta(548)$  and  $\eta'(958)$  belong to the ground state pseudoscalar nonet. As stated in Refs. [45],  $\pi(1300)$ ,  $K(1460)$ ,  $\eta(1295)$ ,  $\eta(1475)$  form the first radial excitation of  $0^-$  meson nonet. The third pseudoscalar nonet is grouped by  $\pi(1800)$ ,  $K(1830)$ ,  $\eta(1760)$ ,  $X(1835)$ . In this paper, we speculate that the fourth and fifth pseudoscalar meson nonets are made by  $\{\pi(2070), K(2150), \eta(4S), \eta(2225)\}$  and  $\{\pi(2360), K(2414), \eta(5S), \eta(2500)\}$ , respectively. Here, the candidates for  $\eta(4S)$  could be  $\eta(2010)$ ,  $\eta(2100)$ ,  $\eta(2190)$ ,  $X(2120)$ ,  $X(2100)$ , while  $\eta(5S)$  could be either  $X(2370)$  or  $\eta(2320)$ . Note that  $K(2414)$  and  $K(2150)$  are predicted particles by using diagonalization of the mass squared matrix and Gell-Mann-Okubo mass formula. Our speculation satisfies the Regge trajectories.

Within this scheme, the strong decay of these states are studied by the flux-tube model.  $X(2100)$  or  $\eta(2100)$  as a  $4^1S_0$  state is undetermined, since the experimental information is not sufficient. The suggested channel of these two states for further experimental studies is  $\pi a_0(1450)$ . We exclude  $\eta(2010)$  and  $\eta(2190)$  to be the

third radial excitation of  $\eta(548)$ .  $X(2120)$  is a good candidate of  $\eta(4S)$ , which agrees with the conclusion in Ref. [1]. In addition,  $\pi(2070)$  and  $\eta(2225)$  can be explained as  $\pi(4S)$  and  $\eta'(4S)$ . The predicted particle  $K(2150)$  is a candidate for  $K(4S)$ , for which its dominant channels  $\pi K^*$ ,  $\rho K$  can be tested in future experiment.

By comparing the theoretical and experimental widths, we find that the candidate for  $\eta(5S)$  can not be  $\eta(2320)$  but  $X(2370)$ . The newly observed  $X(2500)$  can be interpreted as  $\eta'(5S)$ . Moreover, we study the strong decay of  $\pi(2360)$  assuming the quantum number is  $5^1S_0$ , where the calculated width agrees with the experimental one with  $R$  around  $5.51 \text{ GeV}^{-1}$ . The predicted strange meson  $K(2414)$  with quantum number  $5^1S_0$  is also studied. The total width is in the range of  $112.1 \sim 371.8 \text{ MeV}$ , with  $R$  in the range of  $5.0 \sim 5.55 \text{ GeV}^{-1}$ . And we suggest further experiments search for this state via  $\pi K^*$ ,  $\rho K$  channels.

The important information of pseudoscalar states provided by BESIII greatly enriches our knowledge about the light hadron spectrum. Further experimental and

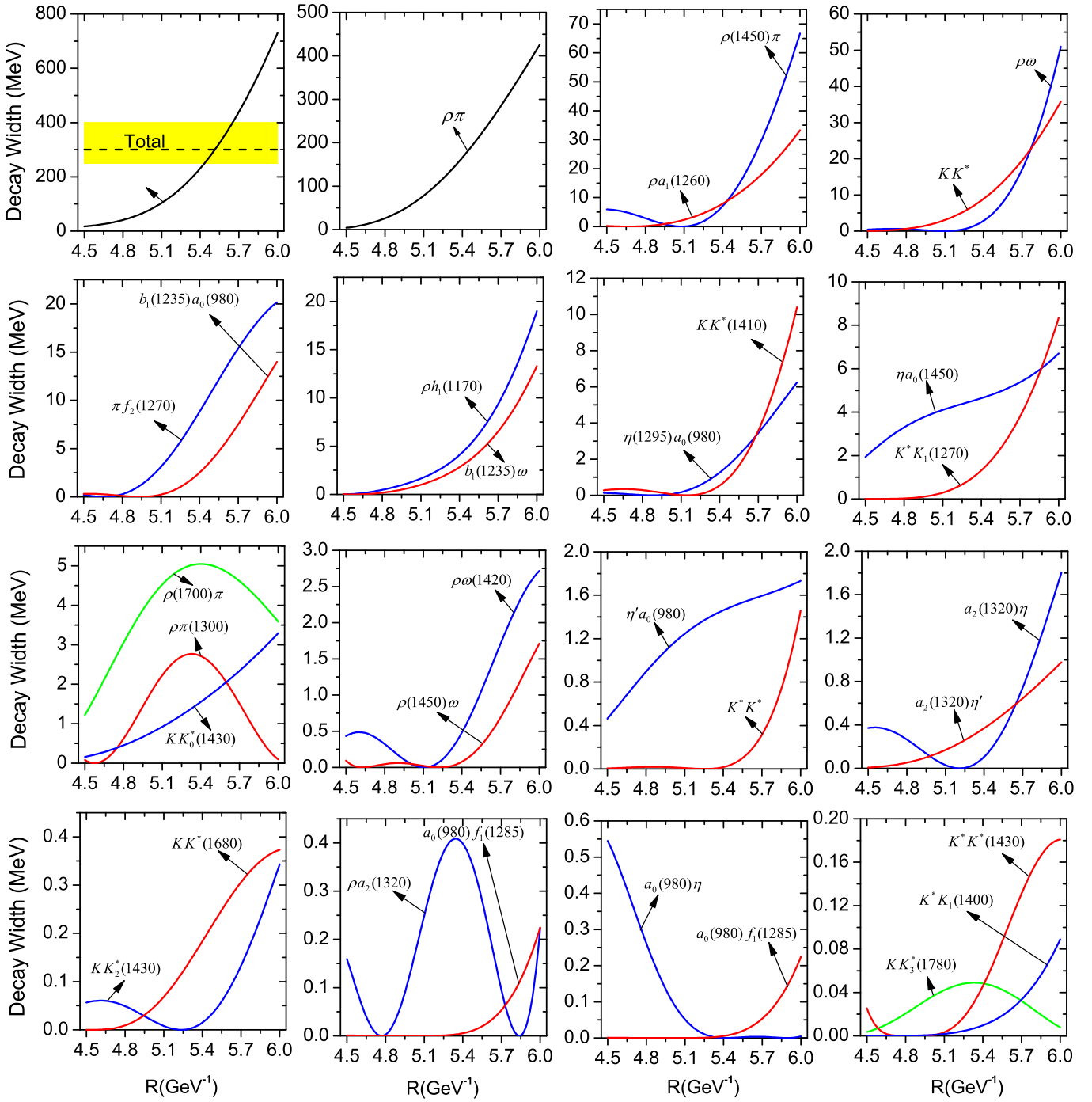


FIG. 7: (color online). The  $R$  dependence of two-body strong decay widths of  $\pi(2360)$  as  $\pi(5S)$  state. The experimental data is marked by the yellow band. Some channels that are tiny, are not drawn up.

theoretical efforts will be helpful to establish new pseudoscalar meson nonets. The predicted behaviors of these discussed states can be tested in near future. We also expect more experimental progresses from BESIII and forthcoming BelleII.

### Acknowledgments

This work is supported in part by National Natural Science Foundation of China under the Grant No. 11222547 and No. 11175073, and the Fundamental Research Funds for the Central Universities. Xiang Liu is also supported by the National Program for Support of Top-notch Young

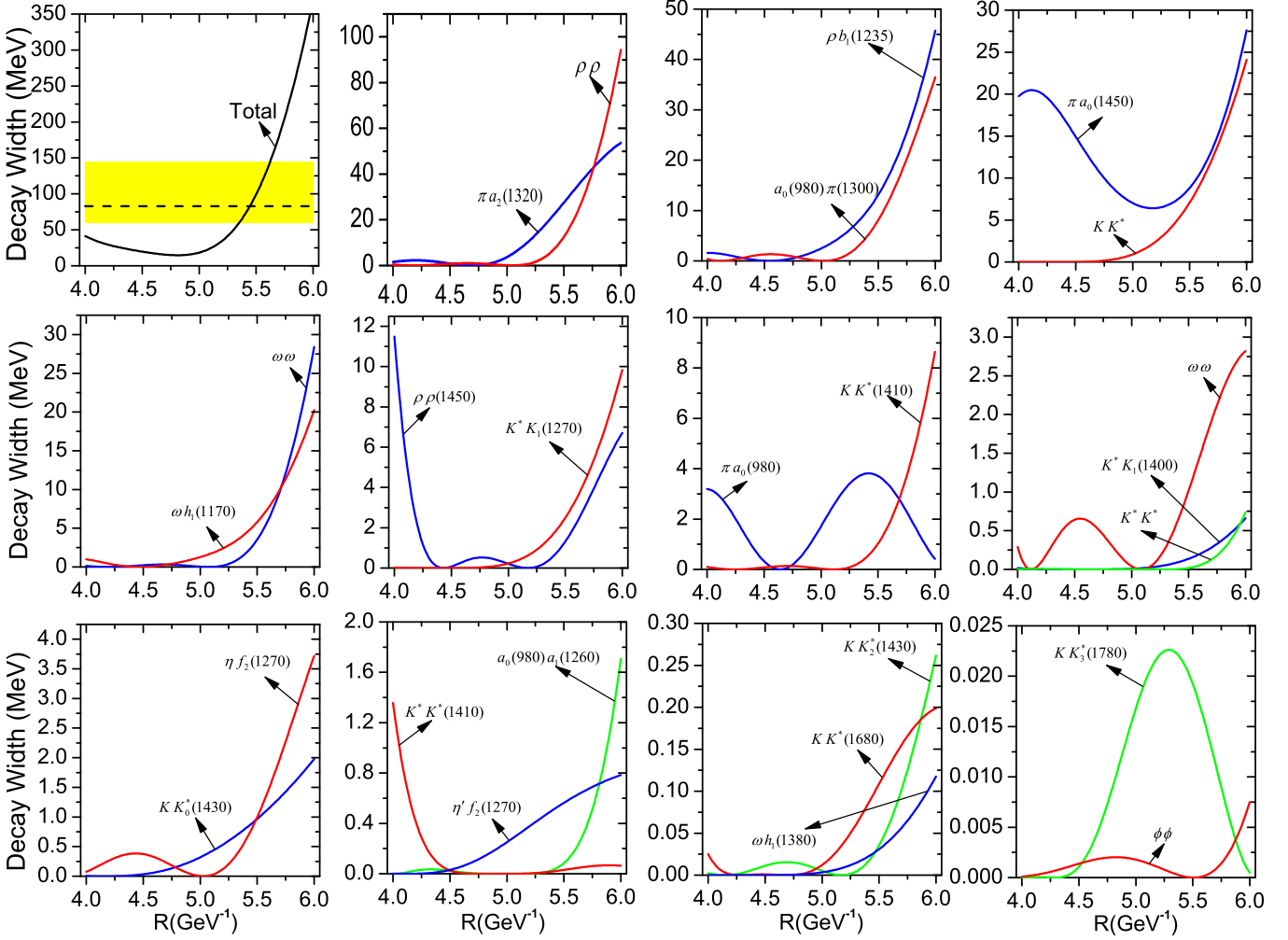


FIG. 8: (color online). The  $R$  dependence of total decay widths and partial two-body decay width of  $X(2370)$  as the fourth radial excitation of  $\eta$ . The experimental data is marked by the yellow band. Some channels that tiny, are not drawn up. Here, the mixing angle we take is  $4.18^\circ$ .

Professionals.

---

[1] J. S. Yu, Z. F. Sun, X. Liu and Q. Zhao, Categorizing resonances  $X(1835)$ ,  $X(2120)$  and  $X(2370)$  in the pseudoscalar meson family, *Phys. Rev. D* **83**, 114007 (2011)

[2] M. Ablikim *et al.* [BESIII Collaboration], Observation of pseudoscalar and tensor resonances in  $J/\psi \rightarrow \gamma\phi\phi$ , *Phys. Rev. D* **93**, 112011 (2016)

[3] M. Ablikim *et al.* [BES Collaboration], Partial wave analysis of  $J/\psi \rightarrow \gamma\phi\phi$ , *Phys. Lett. B* **662**, 330 (2008)

[4] A. V. Anisovich *et al.*,  $I = 0$   $C = +1$  mesons from 1920 to 2410 MeV, *Phys. Lett. B* **491**, 47 (2000)

[5] C. Patrignani *et al.* [Particle Data Group], Review of Particle Physics, *Chin. Phys. C* **40**, 100001 (2016).

[6] C. Shen [BESIII Collaboration], Recent results from BE-SIII, *PoS HQL 2010*, 006 (2010)

[7] D. Bisello *et al.* [DM2 Collaboration], First Observation of Three Pseudoscalar States in the  $J/\psi \rightarrow \gamma\rho\rho$  Decay, *Phys. Rev. D* **39**, 701 (1989).

[8] M. Ablikim *et al.* [BESIII Collaboration], Confirmation of the  $X(1835)$  and observation of the resonances  $X(2120)$  and  $X(2370)$  in  $J/\psi \rightarrow \gamma\pi^+\pi^-\eta'$ , *Phys. Rev. Lett.* **106**, 072002 (2011)

[9] A. V. Anisovich, V. V. Anisovich, V. N. Markov, M. A. Matveev, V. A. Nikonov and A. V. Sarantsev, Radiative decays of quarkonium states, momentum operator expansion and nilpotent operators, *J. Phys. G* **31**, 1537 (2005)

[10] D. M. Li and S. Zhou, Towards the assignment for the  $4^1S_0$  meson nonet, *Phys. Rev. D* **78**, 054013 (2008)

[11] D. M. Li and B. Ma,  $\eta(2225)$  observed by BES Collaboration, *Phys. Rev. D* **77**, 094021 (2008)

[12] A. V. Anisovich, C. A. Baker, C. J. Batty, D. V. Bugg, V. A. Nikonov, A. V. Sarantsev, V. V. Sarantsev and

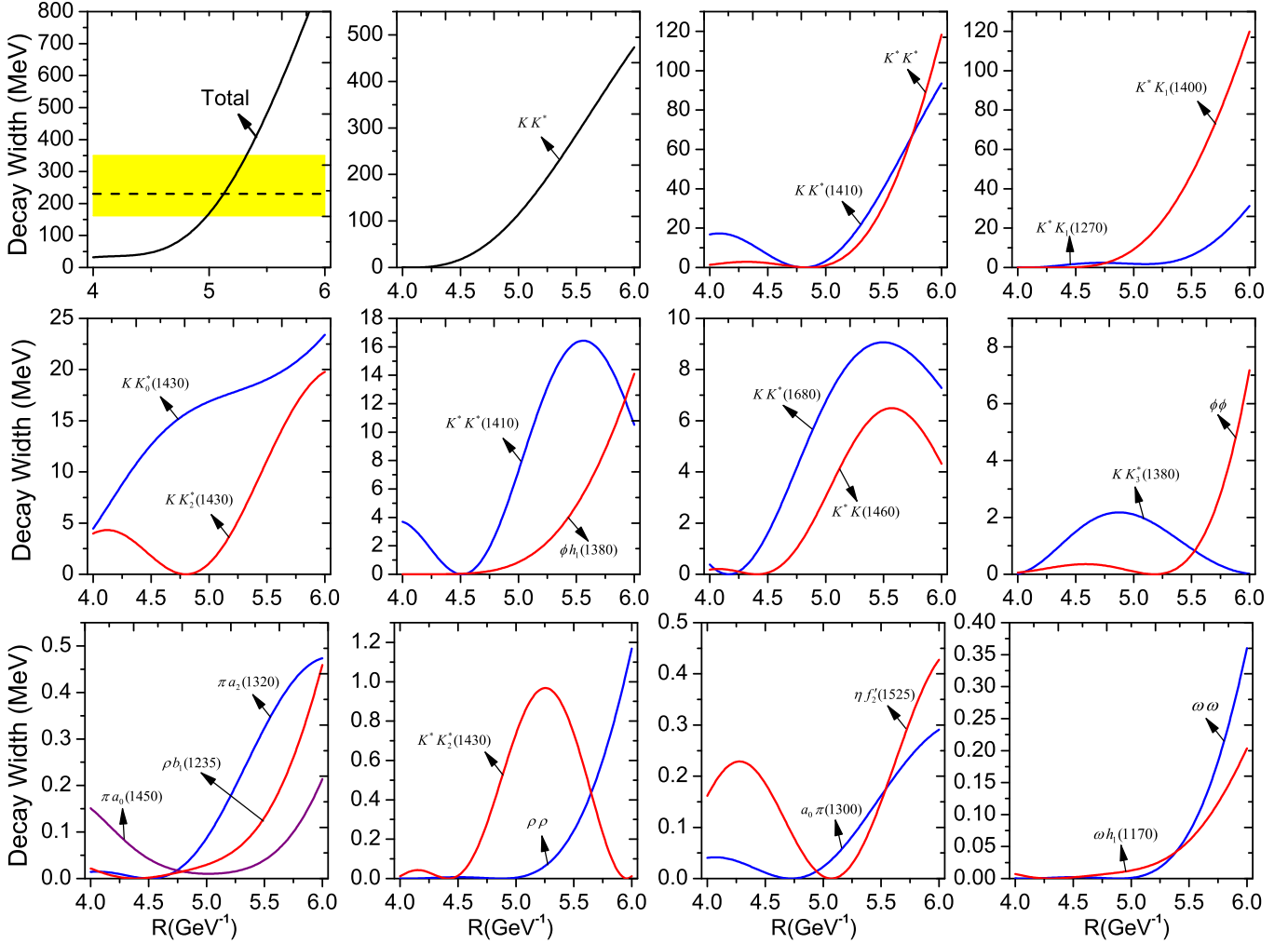


FIG. 9: (color online). The  $R$  dependence of total decay widths and partial two-body decay width of  $X(2500)$  as the fourth radial excitation of  $\eta'$ . The experimental data is marked by the yellow band. Some channels that tiny, are not drawn up. Here, the mixing angle we take is  $4.18^\circ$ .

B. S. Zou, A Study of  $\bar{p}p \rightarrow \eta\eta\eta$  for masses 1960 to 2410 MeV, arXiv:1109.4008 [hep-ex].

[13] J. F. Liu *et al.* [BES Collaboration],  $X(1835)$  and the New Resonances  $X(2120)$  and  $X(2370)$  Observed by the BES Collaboration, Phys. Rev. D **82**, 074026 (2010)

[14] D. M. Li and B. Ma,  $X(1835)$  and eta(1760) observed by BES Collaboration, Phys. Rev. D **77**, 074004 (2008)

[15] L. S. Geng, R. Molina and E. Oset, On the chiral covariant approach to  $\rho\rho$  scattering, arXiv:1612.07871 [nucl-th].

[16] A. Windisch, The analytic properties of the quark propagator from an effective infrared interaction model, arXiv:1612.06002 [hep-ph].

[17] K. Higashijima, Solutions of the Spinor-Spinor Bethe-Salpeter Equation in the Scalar-Vector Sector, Prog. Theor. Phys. **55**, 1591 (1976).

[18] P. Falkensteiner, Matrix Elements and Decays of Baryons in a Bethe-Salpeter Model With Strong Binding, Acta Phys. Austriaca **53**, 175 (1981).

[19] Y. Tomozawa, Normalization of the Three-body Bethe-Salpeter Wave Function for Protons, J. Math. Phys. **24**, 369 (1983).

[20] A. V. Anisovich, C. A. Baker, C. J. Batty, D. V. Bugg, V. A. Nikonov, A. V. Sarantsev, V. V. Sarantsev and B. S. Zou, A partial wave analysis of  $\bar{P}P \rightarrow \eta\eta\pi^0$ , Phys. Lett. B **517**, 273 (2001)

[21] Z. G. Wang, Analysis of the  $X(1835)$  and related baryonium states with Bethe-Salpeter equation, Eur. Phys. J. A **47**, 71 (2011)

[22] S. Chen and J. Ping, Radial excitation states of  $\eta$  and  $\eta'$  the chiral quark model, Chin. Phys. C **36**, 681 (2012)

[23] T. T. Pan, Q. F. L, E. Wang and D. M. Li, Strong decays of the  $X(2500)$  newly observed by the BESIII Collaboration, Phys. Rev. D **94**, no. 5, 054030 (2016)

[24] G. F. Chew and S. C. Frautschi, Regge Trajectories and the Principle of Maximum Strength for Strong Interactions, Phys. Rev. Lett. **8**, 41 (1962).

[25] V. N. Kovalenko, A. M. Puchkov, V. V. Vechernin and D. V. Diatchenko, Restrictions on  $pp$  scattering amplitude imposed by first diffraction minimum data obtained by TOTEM at LHC,

[26] P. R. Page, Excited charmonium decays by flux tube

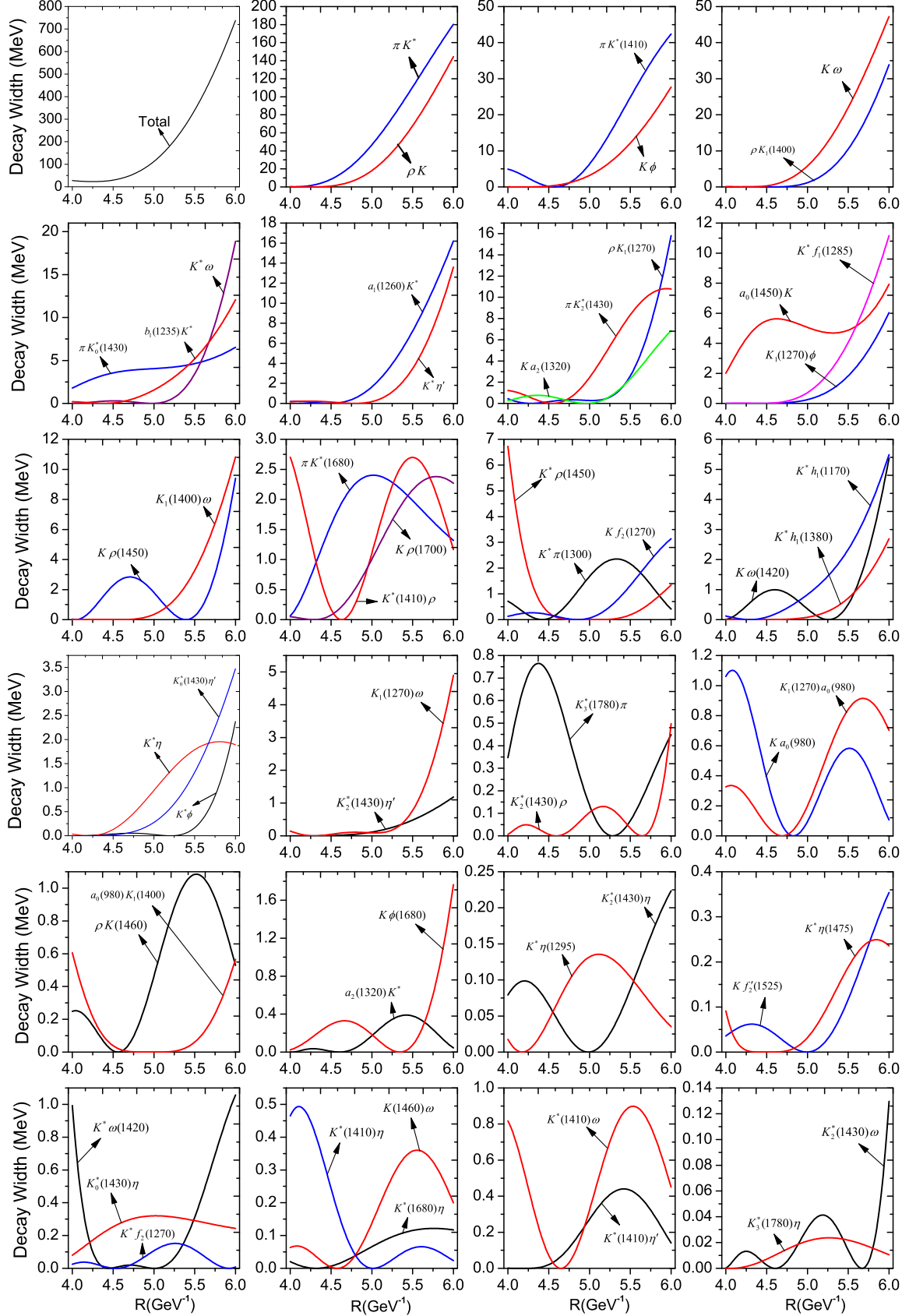


FIG. 10: (color online). The  $R$  dependence of two-body decay widths of  $K(2414)$  as the fourth radial excitation of  $K$ . Some channels that tiny, are not drawn up here.

breaking and the psi-prime anomaly at CDF, Nucl. Phys. B **446**, 189 (1995)

[27] S. Capstick and N. Isgur, Baryons in a Relativized Quark Model with Chromodynamics, Phys. Rev. D **34**, 2809 (1986) [AIP Conf. Proc. **132**, 267 (1985)].

[28] S. Capstick and W. Roberts, Quasi two-body decays of nonstrange baryons, Phys. Rev. D **49**, 4570 (1994)

[29] E. S. Ackleh, T. Barnes and E. S. Swanson, On the mechanism of open flavor strong decays, Phys. Rev. D **54**, 6811 (1996)

[30] A. V. Anisovich, V. V. Anisovich and A. V. Sarantsev, Systematics of  $q\bar{q}$  states in the  $(n, M^2)$  and  $(J, M^2)$  planes, Phys. Rev. D **62**, 051502 (2000)

[31] T. Huang and S. L. Zhu,  $X(1835)$ : A Natural candidate of eta-prime's second radial excitation, Phys. Rev. D **73**, 014023 (2006)

[32] S. Shu, One loop quantum fluctuations to the energy of the non-topological soliton in Friedberg-Lee model,

[33] N. Isgur and J. E. Paton, A Flux Tube Model for Hadrons in QCD, Phys. Rev. D **31**, 2910 (1985).

[34] C. R. Deng, J. L. Ping and F. Wang, Dynamical Study of the Light Scalar Mesons below 1 GeV in a Flux-tube Model, Chin. Phys. C **37**, 033101 (2013)

[35] H. G. Blundell, Meson properties in the quark model: A look at some outstanding problems, hep-ph/9608473.

[36] H. M. Zhao, Z. Q. Zeng, P. N. Shen, Y. B. Ding and X. Q. Li, Possibly stable configurations of  $\Theta^+$  in the flux-tube model, nucl-th/0504053.

[37] P. Geiger and E. S. Swanson, Distinguishing among strong decay models, Phys. Rev. D **50**, 6855 (1994)

[38] D. M. Li and S. Zhou, On the nature of the  $\pi(2)(1880)$ , Phys. Rev. D **79**, 014014 (2009)

[39] R. Kokoski and N. Isgur, Phys. Rev. D **35**, 907 (1987).

[40] F. E. Close and E. S. Swanson, Dynamics and decay of heavy-light hadrons, Phys. Rev. D **72**, 094004 (2005)

[41] Q. T. Song, D. Y. Chen, X. Liu and T. Matsuki, Charmed-strange mesons revisited: mass spectra and strong decays, Phys. Rev. D **91**, 054031 (2015)

[42] S. Godfrey and I. T. Jardine, Nature of the  $D_{s1}^*(2710)$  and  $D_{sJ}^*(2860)$  mesons, Phys. Rev. D **89**, 074023 (2014)

[43] S. Godfrey and N. Isgur, Mesons in a Relativized Quark Model with Chromodynamics, Phys. Rev. D **32**, 189 (1985).

[44] A. V. Anisovich, V. V. Anisovich, V. N. Markov, M. A. Matveev, V. A. Nikonov and A. V. Sarantsev, Radiative decays of quarkonium states, momentum operator expansion and nilpotent operators, J. Phys. G **31**, 1537 (2005)

[45] E. Klemp and A. Zaitsev, Phys. Rept. **454**, 1 (2007) [arXiv:0708.4016 [hep-ph]].

[46] V. V. Anisovich, L. G. Dakhno, M. A. Matveev, V. A. Nikonov and A. V. Sarantsev, Quark-antiquark states and their radiative transitions in terms of the spectral integral equation. III. Light mesons, Phys. Atom. Nucl. **70**, 450 (2007) [Yad. Fiz. **70**, 480 (2007)]

[47] K. Golec-Biernat, S. Jadach, W. Placzek and M. Skrzypek, Solving QCD evolution equations in rapidity space with Markovian Monte Carlo, Acta Phys. Polon. B **39**, 115 (2008) Erratum: [Acta Phys. Polon. **40**, 213 (2009)]

[48] D. V. Bugg, L. Y. Dong and B. S. Zou, The broad  $J^P = 0^-$  meson in  $J/\psi$  radiative decays, Phys. Lett. B **458**, 511 (1999).

[49] N. V. Krasnikov and A. A. Pivovarov, The Use of Finite Energy Sum Rules for the Description of Resonances in QCD, Phys. Lett. **112B**, 397 (1982) [Sov. J. Nucl. Phys. **35**, 744 (1982)] [Yad. Fiz. **35**, 1270 (1982)].

[50] S. G. Gorishnii, A. L. Kataev and S. A. Larin, Next Next-to-leading Perturbative QCD Corrections and Light Quark Masses, Phys. Lett. **135B**, 457 (1984).

[51] D. M. Li, K. W. Wei and H. Yu, A Possible assignment for the ground scalar meson nonet, Eur. Phys. J. A **25**, 263 (2005)

[52] R. Bonnaz and B. Silvestre-Brac, Discussion of the  $^3P_0$  model applied to the decay of mesons into two mesons, Few Body Syst. **27**, 163 (1999).

[53] L. P. He, X. Wang and X. Liu, Towards two-body strong decay behavior of higher  $\rho$  and  $\rho_3$  mesons, Phys. Rev. D **88**, 034008 (2013)

[54] K. Chen, C. Q. Pang, X. Liu and T. Matsuki, Light axial vector mesons, Phys. Rev. D **91**, 074025 (2015)

[55] P. Ghosh, S. Ghosh and N. Bera, Classical and revival time periods of confined harmonic oscillator, Indian J. Phys. **89**, 157 (2014).

[56] A. Kazi, G. Kramer and D. H. Schiller, Decay of the  $\psi(3.1)$  in broken  $SU_4$ , Lett. Nuovo Cim. **15**, 120 (1976).

[57] H. Vogel [CLEO-c Collaboration], Charmonium spectroscopy and decay at CLEO-c, Chin. Phys. C **34**, 621 (2010).

[58] P. Kienle *et al.* [Two-Body-Weak-Decays Collaboration], High-resolution measurement of the time-modulated orbital electron capture and of the  $\beta^+$  decay of hydrogen-like  $^{142}\text{Pm}^{60+}$  ions, Phys. Lett. B **726**, 638 (2013)

[59] S. M. Zebarjad and S. Zarepour, Two-body decay widths of lowest lying and next-to-lowest lying scalar and pseudoscalar mesons in generalized linear sigma model, Int. J. Mod. Phys. A **30**, 1550134 (2015)

[60] H. Hatanaka and K. C. Yang,  $B \rightarrow K_1 \gamma$  Decays in the Light-Cone QCD Sum Rules, Phys. Rev. D **77**, 094023 (2008) Erratum: [Phys. Rev. D **78**, 059902 (2008)]

[61] A. Falvard *et al.* [DM2 Collaboration], Study of Three-body Hadronic  $J/\psi$  Decays, Phys. Rev. D **38**, 2706 (1988).

[62] L. Chen *et al.* [MARK-III Collaboration], An Amplitude analysis of the  $K\bar{K}$  and  $\pi^+\pi^-$  systems ( $M < 2\text{GeV}/c^2$ ) produced in  $J/\psi$  radiative decay, Conf. Proc. C **910812**, 111 (1991).